Power System Technology
ISSN:1000-3673

Received: 06-05-2024 *Revised: 15-06-2024* *Accepted: 28-07-2024*

Presenting a Comprehensive Model to Investigate Phase Transformation and Damage Growth in AISI 304 and AISI 321 At Room Temperature

Reza Barkhordari[1], Mehdi Ganjiani[2] ✉

1- Mechanical Engineering Department, Science and Research branch, Islamic Azad University, Tehran, Iran.
Email: Rbarkhordari28@gmail.com

2- Department of Mechanical Engineering, College of Engineering, University of Tehran, RP.O. Box 11155-4563, Tehran, Iran.
✉Corresponding author's email: Ganjiani@ut.ac.ir.

Abstract:

This research numerically and experimentally investigates damage growth and martensitic phase transformation at room temperature in AISI 304 and AISI 321 stainless steels. Each test comprises two stages: the first stage involves a standard tensile test, and the second stage involves X-ray diffraction to determine the phases present in the stretched sample. In the first stage, tensile tests were conducted under loading-unloading conditions for different displacements, and force-displacement curves were obtained. Damage growth was determined using the unloading slope. Subsequently, the samples were cut using a water jet and subjected to X-ray diffraction to identify the phases present in the sample and their martensitic volume fraction. Using the properties obtained from the experimental tests, a numerical model was developed by implementing the UMAT code in ABAQUS software. This simulation includes two parts: the phase transformation from austenite to martensite and damage growth. In this study, the final models were presented by combining these two models, capable of simultaneously predicting both phenomena at room temperature. Finally, the results of the experimental tests and numerical simulations were compared.

Keywords: Damage, phase transformation, ambient temperature, numerical method, AISI 304, AISI 321

1. Introduction

The 300 series steels are known as austenitic steels. These steels have high stability and weld ability. The concept of stability refers to the resistance of austenitic material to martensitic phase transformation. The most commonly used steels in this series are grades 304 and 321. An important feature of these steels is their high chromium content (16-20%), low carbon content (0.03-0.08%), and significant nickel content (8-14%). Austenitic steels undergo dam-

Power System Technology
ISSN:1000-3673
Received: 06-05-2024 Revised: 15-06-2024 Accepted: 28-07-2024

age due to three major phenomena: strain-induced martensitic phase transformation, soft damage development and yielding. Perdahcıoğlu and Geijselaers (2012).

Damage is a function of plastic strain and the volume fraction of martensite. Based on the type, number and volume fraction of phases, different micro- and macro-mechanical approaches have been proposed for modeling damage and fracture behavior during the plastic deformation of steels. One of the most common methods for calculating the damage parameter is measuring the volume of voids. Another approach involves measuring the reduction in the material's elastic modulus due to tensile testing Ahmedabadi et al. (2016). Models have been developed to predict the behavior of steel materials.

The first phase transformation model was introduced by Garion and Skoczen (2002). In this model, the number of required parameters was minimized due to the difficulty of conducting experiments. The kinetics of the phase transformation was assumed to be linear, and the hardening model was also assumed to increase linearly with the volume fraction of martensite.

Garion and Skoczen (2003) upgraded their previous structural model and presented a model based on the combination of phase transformation and orthotropic damage. The same previous model was used for the phase transformation, but for damage modeling, only damage in the austenitic matrix was considered, and a new soft damage model was introduced. This soft damage model was derived by extending Lemaitre (1985) isotropic soft damage kinetics model to the tensorial state and incorporated into the structural equations using the concept of effective stress.

Lee et al. (2013) introduced a viscoplastic model to investigate crack growth in austenitic steels. In Egner and Ryś (2017) extended the energy equivalence assumption they had applied to damaged material to other dissipative phenomena, such as phase transformation.

Ortwein et al. (2016) applied Lemaitre (1985) model alongside the Garion and Skoczen (2003) to investigate damage development in the torsional twisting of round bars. This study detailed the derivation of the relationships and conducted numerous experiments to determine parameters and martensite content. Damage development and the effect of martensite on increased hardening were qualitatively analyzed. Additionally, a one-dimensional analytical solution was presented, which closely matched the results of the three-dimensional model.

Egner and Ryś (2017) extended the energy equivalence assumption, previously applied to damaged material, to other dissipative phenomena such as phase transformation. They also developed a structural model combining strain-induced phase transformation and damage based on this principle. The potential and state equations in this structural model are similar to those in previous work. However, the dissipation potential and the growth of state variables include the plastic dissipation potential as a von Mises dissipation surface with items related to isotropic and kinematic dynamic recovery, the soft damage dissipation potential modeled as in Saanouni and Devalan (2012), and the damage dissipation potential modeled as

Power System Technology
ISSN:1000-3673
Received: 06-05-2024 Revised: 15-06-2024 Accepted: 28-07-2024

in Al-Rub and Voyiadjis (2003). Additionally, Ryś and Skoczeń (2017) presented a combined model for phase transformation damage. This model describes damage resulting from strain-induced phase transformation and radiation (particle accelerators) that produce nano- or micro-damage. Plastic flow in these materials is typically considered to result from strain due to dynamic evolution and FCC-BCC phase transformation.

Homayounfard et al. (2021) presented a combined model of phase transformation and damage. In this model, they investigated the plastic behavior of AISI 304 at subzero temperatures. The results show that damage initiates at a significant rate during the early stages of phase transformation, but at higher levels of phase transformation, the rate of damage growth decreases until fracture. The presented model accurately predicts the observed damage behavior.

In this study introduced a combined damage-plasticity and martensitic phase transformation model for austenitic steels 304 and 321. Finally, the damage-plasticity and phase transformation results of these steels were compared. Based on these results, damage was calculated by variations in the elastic modulus. The calculation of damage growth on a specific cross-section affects electrical conductivity, acoustic wave propagation, density, hardness, elasticity, and other parameters. Samples were prepared and subjected to tensile tests with loading and unloading cycles to determine the effective elastic modulus at each stage. Subsequently, the phase transformation and martensitic volume fraction of the samples were measured using X-ray diffraction, allowing for a quantitative assessment of damage and martensitic phase fraction and their impact on each other.

2. Theoretical background

The growth of holes at microscopic scales during material fracture, which leads to the weakening of their mechanical properties, is called damage Murakami (2012). Continuous damage mechanics tracks the progression of damage at macroscopic scales within the framework of continuum mechanics. To analyze the effects of microscopic discontinuities in materials (such as voids and impurities) using continuum mechanics, the mechanical effects of the microstructure must first be homogenized and represented as a field to express macroscopic continuity in the material.

2.1. Damage model

In continuous damage mechanics, the damage state is first defined using suitable damage variables. Next, the mechanical behavior of the damaged material and the damage growth rate are described. The Lemaitre (1985) has been employed for this purpose. Additionally, the model by Homayounfard et al. (2021)has been used to describe the hardening behavior. Homogenization methods are omitted in this model. The damage growth equation based on the Lemaitre (1985) is expressed as follows:

Power System Technology
ISSN:1000-3673
Received: 06-05-2024 Revised: 15-06-2024 Accepted: 28-07-2024

$$\dot{D} = -\frac{Y}{S}\dot{\varepsilon}_p H(\varepsilon_p - \varepsilon_D) \tag{1}$$

where H is the step function, ε_P is the plastic strain, and ε_D is the plastic strain threshold for damage. Y is the energy release rate density associated with damage, which is expressed by the following relationship:

$$Y = -\frac{\sigma_{eq}^2}{2E_0(1-D)^2}\left[\frac{2}{3}(1+\upsilon)+3(1+2\upsilon)\left\{\frac{\sigma_H}{\sigma_{eq}}\right\}^2\right] \tag{2}$$

where υ is the Poisson's ratio, σ_{eq} is von Mises effective stress and hydrostatic stress is defined as follows:

$$\sigma_H = \frac{\sigma_{11}+\sigma_{22}+\sigma_{33}}{3} \tag{3}$$

According to the model of Homayounfard et al. (2021), the effect of martensite on the hardening of the material is expressed as follows:

$$R = K(\xi)(\varepsilon_p)^n \tag{4}$$

$$K(\xi) = K_0 + K_1\xi \tag{5}$$

The parameters $K(\xi)$ and n are the hardening coefficient and the hardening exponent, respectively, and R represents the hardening value of the material. According to equation(5), the hardness coefficient K changes linearly with the amount of martensite. For a simple tensile test, equation (2) substituted into equation (1) and, after integration, the damage equation is obtained as equation

$$D = \frac{R^2}{2E_0 S}(\varepsilon_p - \varepsilon_D) \tag{6}$$

2.2. Phase transformation model

Series 300 steels are in the face-centered cubic (FCC) austenite phase at room temperature. This phase can transform into body-centered tetragonal (BCT) ferrite (α') or hexagonal ε. The ε phase can be considered an intermediate phase during the $\gamma \to \alpha'$ transformation Reed (1983). This phase forms at strains of approximately 7 to 15%, after which its volume fraction decreases Lebedev and Kosarchuk (2000). Consequently, martensite is generally considered to be in the (BCC) phase. The phase transformation $\gamma \to \alpha'$ behavior was described by Olson and Cohen (1975). The growth of the martensite fraction (ξ) with respect to plastic strain, represented as an elliptical curve, is shown in Figure 1. The relationship for the growth of the martensite volume fraction with plastic strain is defined by the equation from Shin et al. (2001). As follows:

$$\xi = \xi^L\left[1-\exp\left\{-\beta(\varepsilon_p - \varepsilon_\xi)^\alpha\right\}\right] \tag{7}$$

where ξ^L is the saturation level of martensite, ε_ξ is the strain at which phase transformation begins, β and α are constant coefficients. Based on this, the yield surface can be defined

Power System Technology
ISSN:1000-3673
Received: 06-05-2024 Revised: 15-06-2024 Accepted: 28-07-2024

using the effective stress σ_{eq} and effective isotropic hardening R.

$$\sigma_{eq} = \sigma_y^0 + R \tag{8}$$

In this context, σ_y^0 is the yield stress of the material, while σ_{eq} and R are defined as follows:

$$\sigma_{eq} = \frac{\sigma_{eq}}{1-D} \tag{9}$$

$$R = \frac{R}{1-D} \tag{10}$$

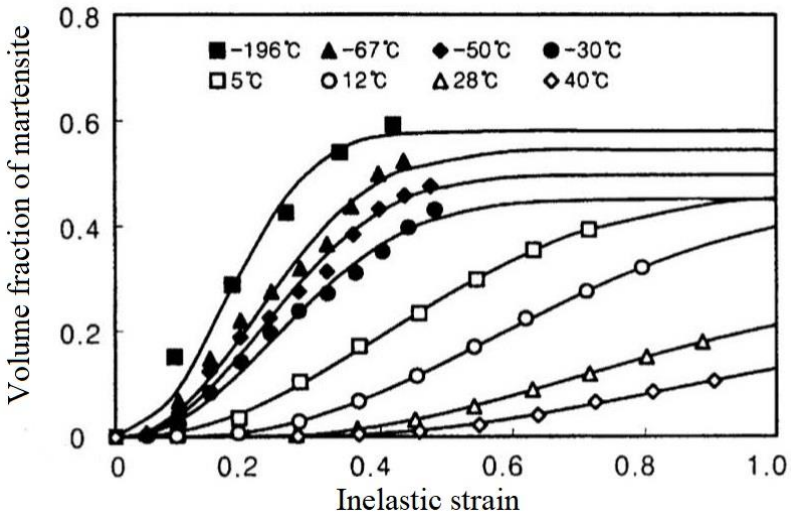

Figure 1.Volume fraction of Martensite growth in terms of plastic strain Shin et al. (2001).

3. Experimental analysis

Experimental tests were conducted to determine phase transformation induced by plastic strain and the development of damage in 304 and 321 steels. These tests involved uniaxial tension. The samples were stretched to displacements of 3, 4, 6, 8, and 12 mm. After stretching, the samples were held in position for five seconds and then unloaded. These tests were conducted at room temperature. Finally, to determine the amount of martensite at each strain, the samples underwent X-ray diffraction tests. To ensure the accuracy of the experimental results, each test was repeated twice.

3.1. Material and method

The sample specifications were chosen according to standard E8M-09 Astm (2016), as shown in Figure 2 and Tables 1.

Power System Technology
ISSN:1000-3673

Received: 06-05-2024 Revised: 15-06-2024 Accepted: 28-07-2024

Table 1. The chemical composition of AISI 304 and AISI 321.

	Si	C	Mn	P	Ti	S	Cr	Ni	Mo	Ti
AISI304	**0.48**	**0.051**	**1.71**	**0.03**	**0.011**	**0.026**	**18.4**	**11**	**0.421**	**0.007**
AISI321	**0.381**	**0.097**	**1.77**	**0.042**	**0.008**	**0.021**	**18.9**	**12**	**0.521**	**0.005**

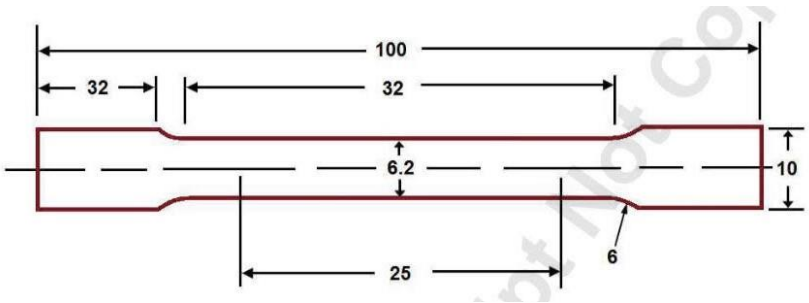

Figure 2. The geometry of the simple dimensions in (mm) for tensien tests.

3.2. Tensile test

The device used in this study was the Santam-STM-250. This machine can apply up to 250 (KN) of force to the sample. The range of the upper movable clamp's displacement rate is from 0.001 to 250 $mm/\min$. The loadcells of this device are in class 0.5, with a maximum error of 0.5% of the reading within 2% to 100% of the loadcells capacity, according to ISO7500 (TC, 2009) and EN10002 standards STANDARD (2010). A picture of this device is shown in Figure 3. According to the standard, the estimated displacement rate of the clamp was set at $0.75\ mm/\min$.

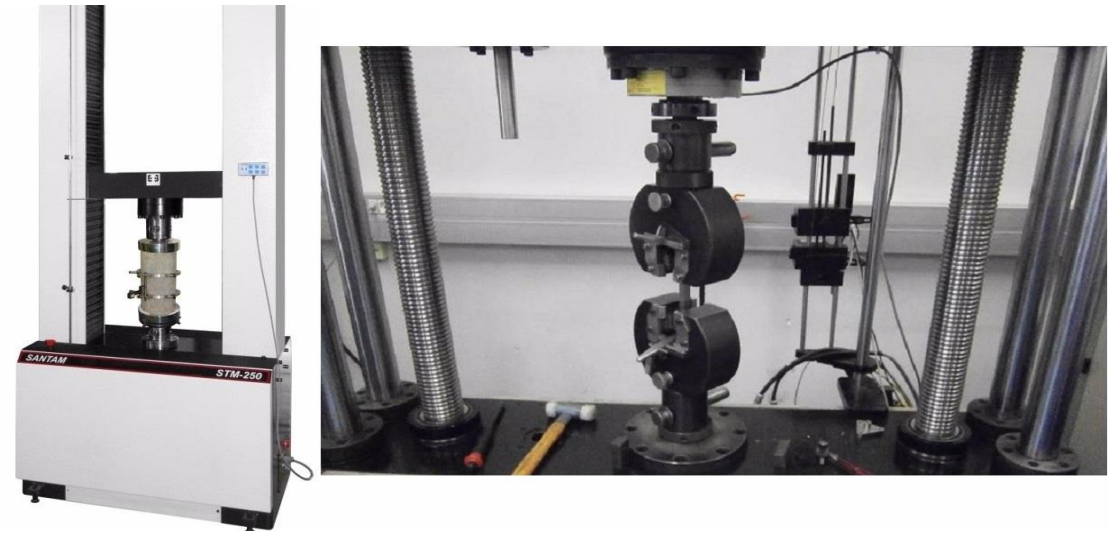

Figure 3. Test setup for tensile test.

Power System Technology
ISSN:1000-3673

Received: 06-05-2024 Revised: 15-06-2024 Accepted: 28-07-2024

3.3. Tensile test results

The purpose of this test was to obtain the stress-strain curve, which contains information about the material's elastic-plastic deformation and damage properties. To determine the damage parameter, the samples were unloaded. Parameters such as the elastic modulus E_0, yield stress σ_y^0, and damage variable D were derived from these curves. The engineering stress-strain curves of the austenitic steels are shown in Figure 4. According to Figure 4, the elastic modulus values at each strain were obtained using the slope of the unloading curve. This value represents the elastic modulus of the material in the presence of damage $E(D)$. By knowing the initial (undamaged) elastic modulus E_0, the damage parameter can be calculated using the following relationship. Finally, the damage versus plastic strain curve is shown in Figure 5.

$$D = 1 - \frac{E(D)}{E_0} \tag{11}$$

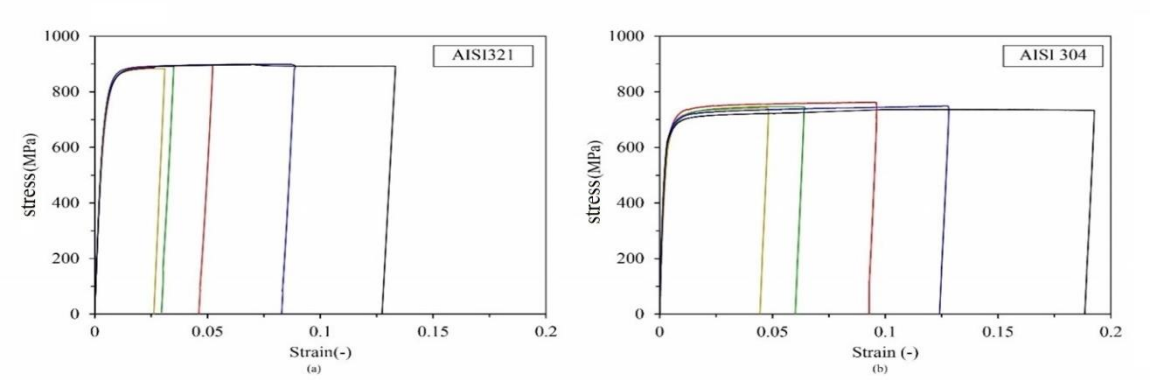

Figure 4. Engineering stress-strain curve for (a)AISI 321 (b) AISI 304

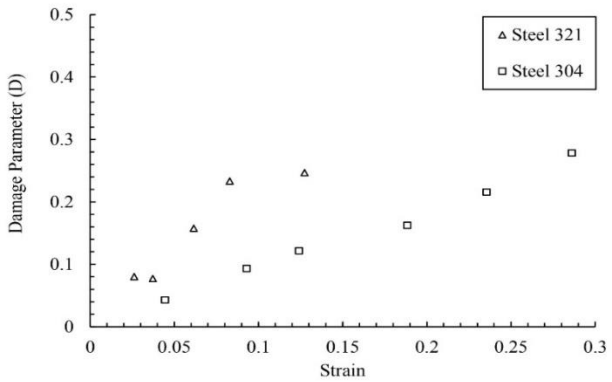

Figure 5. Damage parameter against the Strain.

Power System Technology
ISSN:1000-3673

Received: 06-05-2024 *Revised: 15-06-2024* *Accepted: 28-07-2024*

3.4. X-Ray Diffraction (XRD) test

To calculate the volume fraction of martensite at various displacements (4, 6, 8, 10, and 12 mm), X-ray diffraction tests were conducted. The X-ray diffraction pattern is a quick analytical method used to identify material types as well as their phases and crystalline properties. This test was performed on samples stretched at room temperature. For this purpose, a small piece was taken from the middle of the test samples, and after preparation, an X-ray diffraction test was conducted. The results for the 12 mm displacement are shown in Figure 6. The vertical axis of this graph represents the intensity of the X-ray reflection from the sample, while the horizontal axis shows twice the angle of the beam relative to the horizon. Peaks in this graph indicate specific phases within the material. The cubic face-centered austenite phase and the martensite phase were identified in the 304 and 321 steel samples. The three-digit numbers in parentheses next to each phase type indicate the plane in which the phase is located. These planes will be used to determine the volume fraction of martensite. In the equation(12), I' represents the intensity of the X-ray reflected from the sample. The phase plane and the type of phase present in the austenitic stainless steel are identified for each peak. According to equation(12), the martensite volume fraction versus plastic strain for various displacements and for both tests is shown in Figure 7. In this figure, the horizontal axis represents the plastic strain, and the vertical axis represents the martensite volume fraction in the stretched sample. Based on the X-ray diffraction patterns, the martensite volume fraction ξ in all five displacement cases can be easily calculated using equation(12) .Naghizadeh and Mirzadeh (2016):

$$\xi = \frac{I'_{(211)\alpha'}}{I_{(211)\alpha'} + 0.65\,(I_{(311)\gamma} + I_{(220)\gamma})} \tag{12}$$

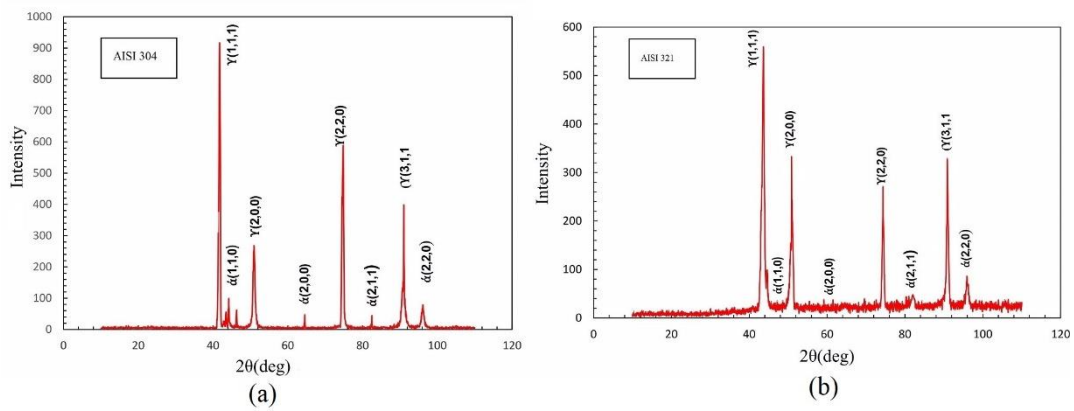

Figure 6. XRD test result for a sample with. $\varepsilon^p = 0.085$ (a)AISI 304 (b) AISI 321

Power System Technology
ISSN:1000-3673

Received: 06-05-2024 Revised: 15-06-2024 Accepted: 28-07-2024

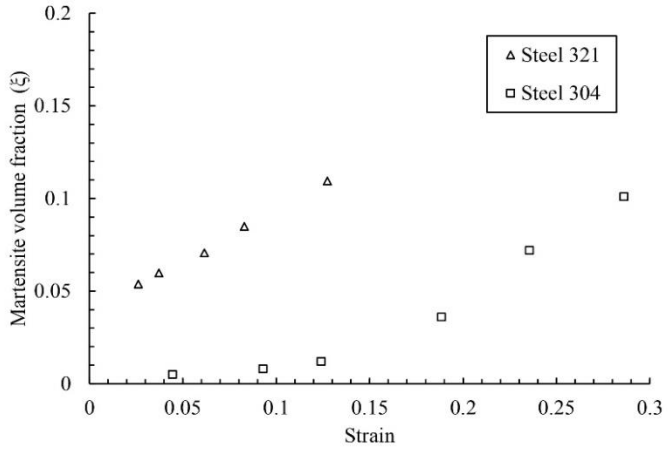

Figure 7.Martensite volume fraction against the plastic strain.

4. Parameter Identification procedure

The material parameters involved in the models used can be identified through loading-unloading tensile tests and evaluating the X-ray diffraction test results of unloaded samples. ABAQUS software was used as a numerical simulation tool. The following steps were taken to calibrate the model, and the results are listed in Table 2.

1. To obtain the parameters ξ^L, α, β and ε_ξ, the model was calibrated with the data from the X-ray diffraction tests.
2. Using the experimental unloading data and the stress values corresponding to the damage model, assuming $\varepsilon_D = \varepsilon_\xi$ and the parameters S and ε_D were determined.
3. The tensile test results before the phase transformation began were used to identify the parameters K_0, n and σ_y^0.
4. The parameter K_1 was calculated by fitting the stress-strain curve.

Table 2. Material parameter for investigated steel.

	E_0(GPa)	υ	σ_y^0(GPa)	$\varepsilon_D = \varepsilon_\xi$	ξ^L	β	α	K_0(GPa)	n	K_1(GPa)	S(GPa)
AISI304	**200**	**0.3**	**700**	**0.001**	**0.05**	**1**	**1.45**	**400**	**0.6**	**15000**	**2**
AISI321	**200**	**0.3**	**860**	**0.001**	**0.05**	**3**	**1.45**	**700**	**0.6**	**17000**	**1.3**

5. Comparison of experimental and numerical Results

By matching the numerical and experimental results, the numerical method was validated, and the phase transformation and damage parameters for all three materials were analyzed and compared. ABAQUS software was used for numerical simulation, with the von Mises

Power System Technology
ISSN:1000-3673
Received: 06-05-2024 Revised: 15-06-2024 Accepted: 28-07-2024

criterion chosen as the yield surface. The UMAT code was implemented in ABAQUS using inputs obtained from the experimental test results. Using the constants from Table 2, stress-strain curves for all three materials were plotted in Figure 8. As shown in Figure 8, all three curves demonstrate a good fit between numerical and experimental results. Figure 9 shows the martensite volume fraction for all three materials during the experimental tests. The numerical model for all three materials indicates zero phase transformation at the beginning of the curve, with the martensite volume fraction gradually increasing with the amount of plastic strain. Overall, the phase transformation in steel 321 is comparable to that in steel 304.Figure 10 presents the numerical and experimental damage values versus plastic strain. According to the graph in Figure 10, the critical damage value (failure point) is approximately 0.28 for steel 304, 0.34 for steel 321. Additionally, steel 304 can endure more strain before failure.

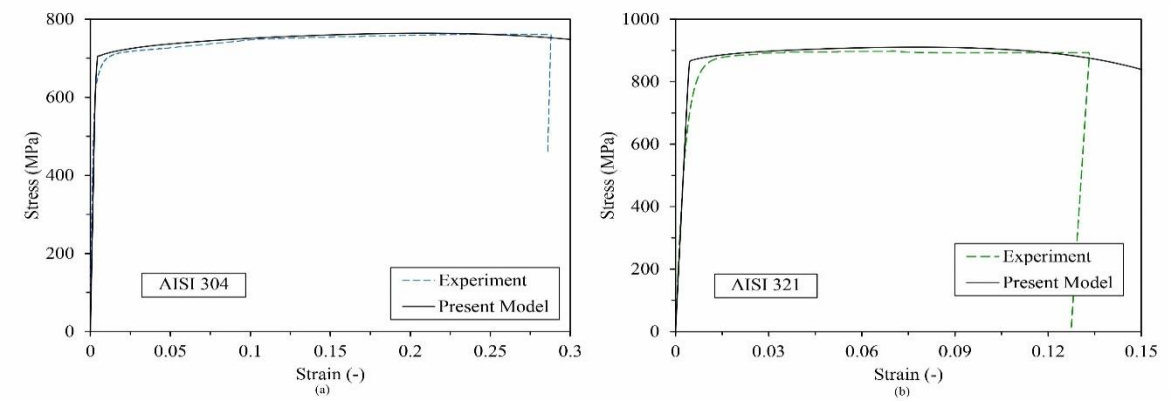

Figure 8.Stress-Strain curve of the present model (a)AISI 304 (b) AISI 321.

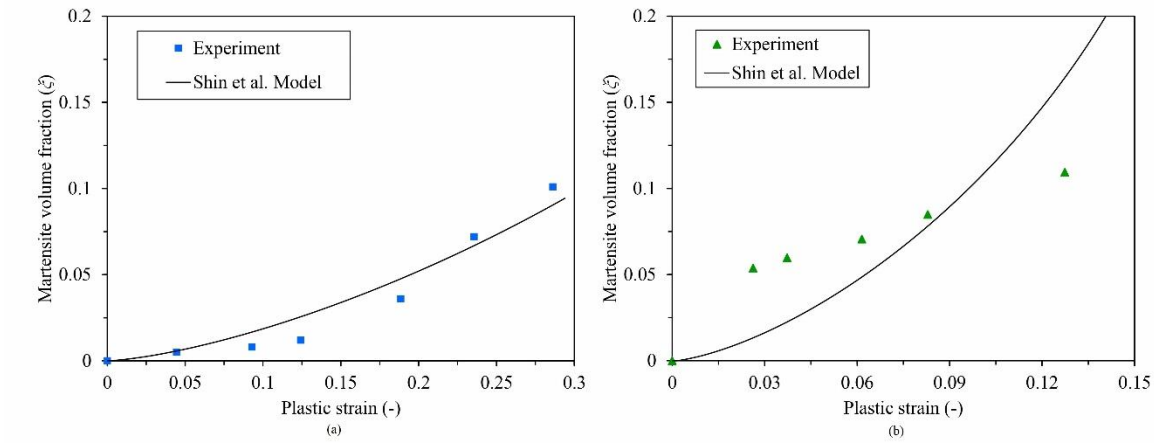

Figure 9. Martensite volume fraction against the plastic strain (a)AISI 304 (b) AISI 321.

Power System Technology
ISSN:1000-3673

Received: 06-05-2024 Revised: 15-06-2024 Accepted: 28-07-2024

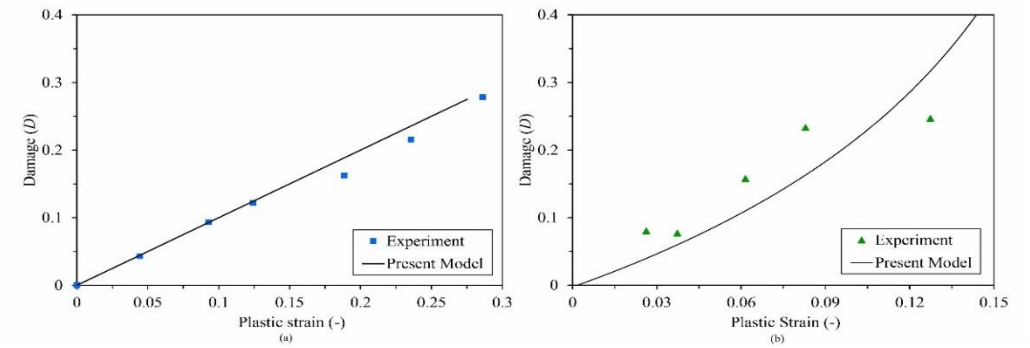

Figure 10. Damage evolution against the plastic strain (a)AISI 304 (b) AISI 321.

6. Conclusion

In this study, the damage and the amount of martensitic phase transformation for austenitic steels 304 and 321 at room temperature were examined. The material properties were determined using tensile test results. X-ray diffraction tests identified the phases within the material and determined the martensite volume fraction at various strains. The material parameters extracted from experimental tests were used as inputs for numerical simulations. The UMAT code was implemented in ABAQUS for the simulations, and the experimental results were compared with the simulation results. The following conclusions were drawn from the comparison and analysis of the results:

1. Martensitic phase transformation due to plastic strain occurs at room temperature, but the amount is negligible.
2. The martensite volume fraction in steel 304 is lower than in the other steel, indicating that steel 304 is more resistant to martensitic phase transformation compared to steels 321. Therefore, when higher ductility and austenite phase presence are desired, steel 304 is preferable over the 321 steels.
3. The rate of damage growth, according to the damage charts, is higher in steel 321 than in the other materials, meaning more damage is observed at lower strains.
4. A direct relationship between the rate of damage growth and the martensite volume fraction in these two materials was also observed from the experimental data.

References

1. Ahmedabadi, P. M., Kain, V., & Agrawal, A. (2016). Modelling kinetics of strain-induced martensite transformation during plastic deformation of austenitic stainless steel. *Materials & Design*, *109*, 466-475.
2. Al-Rub, R. K. A., & Voyiadjis, G. Z. (2003). On the coupling of anisotropic damage and plasticity models for ductile materials. *International Journal of Solids and Structures*, *40*(11), 2611-2643.
3. Astm, I. (2016). ASTM E8/E8M-16a: standard test methods for tension testing of metallic materials. *West Conshohocken, PA, USA: ASTM International*.

Power System Technology
ISSN:1000-3673

Received: 06-05-2024 Revised: 15-06-2024 Accepted: 28-07-2024

4. Egner, H., & Ryś, M. (2017). Total energy equivalence in constitutive modeling of multidissipative materials. *International Journal of Damage Mechanics*, *26*(3), 417-446.
5. Garion, C., & Skoczen, B. (2002). Modeling of plastic strain-induced martensitic transformation for cryogenic applications. *J. Appl. Mech.*, *69*(6), 755-762.
6. Garion, C., & Skoczen, B. (2003). Combined model of strain-induced phase transformation and orthotropic damage in ductile materials at cryogenic temperatures. *International Journal of Damage Mechanics*, *12*(4), 331-356.
7. Homayounfard, M., Ganjiani, M., & Sasani, F. (2021). Damage development during the strain induced phase transformation of austenitic stainless steels at low temperatures. *Modelling and Simulation in Materials Science and Engineering*, *29*(4), 045004.
8. Lebedev, A., & Kosarchuk, V. (2000). Influence of phase transformations on the mechanical properties of austenitic stainless steels. *International Journal of Plasticity*, *16*(7-8), 749-767.
9. Lee, C.-S., Yoo, B.-M., Kim, M.-H., & Lee, J.-M. (2013). Viscoplastic damage model for austenitic stainless steel and its application to the crack propagation problem at cryogenic temperatures. *International Journal of Damage Mechanics*, *22*(1), 95-115.
10. Lemaitre, J. (1985). A continuous damage mechanics model for ductile fracture.
11. Murakami, S. (2012). *Continuum damage mechanics: a continuum mechanics approach to the analysis of damage and fracture* (Vol. 185). Springer Science & Business Media.
12. Naghizadeh, M., & Mirzadeh, H. (2016). Microstructural evolutions during annealing of plastically deformed AISI 304 austenitic stainless steel: martensite reversion, grain refinement, recrystallization, and grain growth. *Metallurgical and Materials Transactions A*, *47*, 4210-4216.
13. Olson, G., & Cohen, M. (1975). Kinetics of strain-induced martensitic nucleation. *Metallurgical transactions A*, *6*, 791-795.
14. Ortwein, R., Ryś, M., & Skoczeń, B. (2016). Damage evolution in a stainless steel bar undergoing phase transformation under torsion at cryogenic temperatures. *International Journal of Damage Mechanics*, *25*(7), 967-1016.
15. Perdahcıoğlu, E., & Geijselaers, H. J. (2012). A macroscopic model to simulate the mechanically induced martensitic transformation in metastable austenitic stainless steels. *Acta Materialia*, *60*(11), 4409-4419.
16. Reed, H. (1983). Martensitic transformations in fe-cr-ni stainless steels. In *Austenitic Steels at Low Temperatures* (pp. 41-67). Springer.
17. Ryś, M., & Skoczeń, B. (2017). Coupled constitutive model of damage affected two-phase continuum. *Mechanics of Materials*, *115*, 1-15.
18. Saanouni, K., & Devalan, P. (2012). Thermomechanically-Consistent Modeling of the Metals Behavior with Ductile Damage. *Damage Mechanics in Metal Forming*, 63-242.
19. Shin, H. C., Ha, T. K., & Chang, Y. W. (2001). Kinetics of deformation induced martensitic transformation in a 304 stainless steel. *Scripta Materialia*, *45*(7), 823-829.
20. STANDARD, B. (2010). Metallic materials—Tensile testing. In: GB.
21. TC, I. (2009). Metallic Materials–Tensile Testing–Part 1: Method of Test at Room Temperature.